Influence of centrifugal forces on phase structure in partially saturated media

Robert M. Holt,[1] Robert J. Glass,[2] John M. Sigda,[3] and Earl D. Mattson[4]

Received 16 March 2003; revised 10 May 2003; accepted 15 May 2003; published 8 July 2003.

[1] Centrifugal methods are gaining increased attention for use in hydrologic experiments within partially saturated media. Through use of a Modified Invasion Percolation (MIP) model, we examine the influence of a stabilizing centrifugal (buoyancy) force on the invasion of a light non-wetting fluid (e.g., air) into a heterogeneous porous media initially saturated with a denser, wetting fluid (e.g., water). Results show that while capillary heterogeneity controls phase structure outside of a centrifugal field, the influence of capillary heterogeneity varies with angular velocity in a centrifugal field. As the angular velocity is increased, the invasion processes and phase structure become increasingly insensitive to heterogeneity, regardless of its style or orientation. Because phase structure critically influences flow processes and petrophysical properties (pressure-saturation, relative permeability, electrical resistivity, etc.), the design of centrifugal experiments must carefully consider this interplay between capillary heterogeneity and centrifugal force. *INDEX TERMS:* 1875 Hydrology: Unsaturated zone; 1829 Hydrology: Groundwater hydrology; 1894 Hydrology: Instruments and techniques. **Citation:** Holt, R. M., R. J. Glass, J. M. Sigda, and E. D. Mattson, Influence of centrifugal forces on phase structure in partially saturated media, *Geophys. Res. Lett.*, *30*(13), 1692, doi:10.1029/2003GL017340, 2003.

1. Introduction

[2] Centrifugal methods are capable of greatly reducing equilibrium times in experiments conducted within partially saturated porous media. Thus, a variety of small-scale centrifugal methods have been developed for measuring hydraulic properties, including pressure-saturation relationships [*Hassler and Brunner*, 1945; *Forbes*, 1994], relative permeability [*Nimmo et al.*, 1987; *Conca and Wright*, 1992], and transport parameters [*Conca and Wright*, 1990; *Gamerdinger and Kaplan*, 2000]. These methods, particularly those for measuring pressure-saturation and relative permeability, are being increasingly applied in practice. Additionally, large-scale geotechnical centrifuges are gaining popularity for studies of multiphase flow and transport processes in dimensionally scaled systems [e.g., *Savvidou and Culligan*, 1998; *Griffioen and Barry*, 1999; *Levy et al.*, 2002].

[3] The assumption that centrifugal forces are similar to gravity forces [e.g., *Hassler and Brunner*, 1945; *Nimmo et al.*, 1987; *Levy et al.*, 2002] is implicit in many centrifuge applications. Both gravity and centrifugal forces create buoyancy effects that can stabilize or destabilize the displacements of immiscible fluids having differing densities. However, unlike gravity forces, centrifugal forces are non-linear, increase with the square of radial distance from the axis of rotation, and vary with the applied angular velocity. Under unsaturated or two-phase flow conditions, the structure of the phases within a porous media critically controls many processes (e.g., flow pathways, solute transport, etc.) and petrophysical properties (e.g., pressure-saturation, relative permeability, electrical resistivity, etc.). For understanding gained from experiments in centrifuges to have relevance or be properly interpreted, one must consider the influence of centrifugal forces on phase structure.

[4] In this paper we illustrate the influence of centrifugal forces on phase structure in the simplest of two-phase experiments, the stabilized displacement of a denser wetting phase (e.g., water) by a lighter non-wetting phase (e.g., air) within a heterogeneous porous medium. Such an experiment, run to equilibrium, is often used to measure drainage curves in samples taken from the field. We model this displacement by adapting a Modified Invasion Percolation (MIP) approach, such as used by others [e.g., *Kueper and McWhorter*, 1992; *Ioannidis et al.*, 1996; *Ewing and Berkowitz*, 1998; *Glass et al.*, 2001], to include both capillary forces and a stabilizing centrifugal force. In addition to a simple random, uncorrelated, heterogeneous capillary field, we also consider the additional influence of spatial structure in context of the ubiquitous layering found in nature. Our results show that both the invasion order and the resulting phase structures vary significantly with centrifugal force. At low angular velocities, the phase structure is similar to that produced by capillary invasion alone and is critically controlled by capillary heterogeneity. However, as the angular velocity increases, the invading front becomes increasingly smooth and insensitive to capillary heterogeneity. This strong influence on phase structure has profound implications for the design and interpretation of centrifuge experiments.

2. Modified Invasion Percolation Model

[5] An MIP approach is used to simulate invasion of a light non-wetting fluid (air) into a medium initially saturated with a dense wetting fluid (water) under the combined influence of capillary and centrifugal driven buoyancy forces. Besides the inclusion of centrifugal forces, the

[1]Department of Geology and Geological Engineering, The University of Mississippi, University, Mississippi, USA.
[2]Flow Visualization and Processes Laboratory, Sandia National Laboratories, Albuquerque, New Mexico, USA.
[3]New Mexico Bureau of Geology and Mineral Resources, New Mexico Institute of Mining and Technology, Albuquerque, New Mexico, USA.
[4]Geosciences Research Department, Idaho National Engineering and Environmental Laboratory, Idaho Falls, Idaho, USA.

0094-8276/03/2003GL017340$05.00

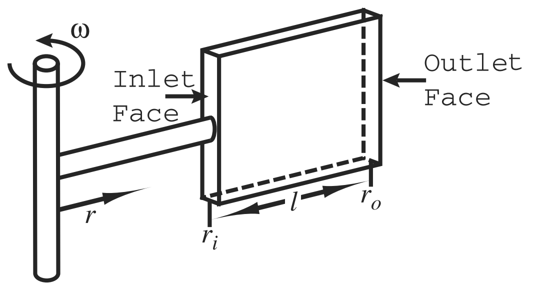

Figure 1. Centrifuge system geometry for measuring drainage curves. Inlet and outlet faces are open to the atmosphere. All other faces are closed and are considered no flow boundaries.

current MIP differs from Invasion Percolation (IP) [e.g., *Wilkinson and Willemsen*, 1983] through the definition of macro, near-pore scale capillarity. Here, individual pore throats and necks are not considered. Instead, a near pore-scale block is defined and characterized by a local threshold spanning pressure (a local block-scale breakthrough pressure) that represents the behavior of the subscale network [e.g., *Glass et al.*, 2001]. The model domain is discretized into an array of grid blocks with assigned spanning pressures. An invasion pressure for each block is then determined by the sum of spanning pressure and centrifugal forces:

$$P_I^* = P_s^* + \frac{\Delta\rho\omega^2}{2} r^2 \quad (1)$$

where P_s^* is the capillary spanning pressure ($ML^{-1}T^{-2}$), $\Delta\rho = \rho_{defender} - \rho_{invader}$ is the difference in densities of the defending and invading phases (ML^{-3}), ω is the angular velocity (T^{-1}), and r is the grid-block radial coordinate (L). For non-wetting phase invasion, P_s^* is intrinsically positive.

[6] In a centrifugal system configured to measure drainage curves (Figure 1), both the inflow face at r_i (L), and the outflow face at r_o (L), are open. Water exits the outflow face by 'falling' through air, and thus the capillary pressure at the outflow face is constrained to be zero so that the last term in (1) becomes $\Delta\rho\omega^2(r^2 - r_i^2)/2$. For this situation, we can write a dimensionless invasion pressure equation as:

$$P_I = P_s + A_V \frac{R(R+2)}{l(l+2)} \quad (2)$$

where spanning pressures have been normalized by the mean value $\langle P_s^* \rangle$, radial position is given by $R = (r - r_i)/r_i$, system length by $l = (r_o - r_i)/r_i$, and A_V is the dimensionless angular velocity number defined as:

$$A_V = \frac{\Delta\rho\omega^2 (r_o^2 - r_i^2)}{2\langle P_s^* \rangle} \quad (3)$$

and reflects the strength of the centrifugal pressure that drives invasion. Like the Bond number in gravitational fields, A_V is a ratio of buoyancy to capillary forces for a centrifugal field. However it increases with radial position r_i and applied angular velocity ω.

[7] MIP is implemented on a field (or network) of prescribed capillary spanning pressures. Non-wetting phase invasion proceeds from the system inlet toward the outlet according to an IP algorithm that implements equation (2). The IP algorithm selects the block connected to the growing cluster with the lowest invasion pressure and invades it. This process continues until blocks along the active interface no longer can be can be invaded at the imposed external capillary pressure or centrifugal force. In absence of centrifugal forces ($A_V = 0$), the invasion pressure history under imposed external capillary pressure directly determines the capillary pressure-wetting phase saturation [$P_c(S_w)$] relationship for drainage. However, when $A_V \neq 0$, this is not the case.

3. Illustrative Simulations

[8] To illustrate the influence of centrifugal forces on phase structure in context of capillary heterogeneity, we consider the case $l = 1$ (i. e., $r_o = 2r_i$), representative of many sample scale experiments. We populate a two-dimensional field of gridblocks (128 by 128) with P_s chosen from a logarithmic distribution (geometric mean of 1.0, variance of $\ln(P_s)$ of 1.0). The field (Figure 2 column A) is either spatially uncorrelated or is correlated to form microlayering using a FFT method and a standard two-dimensional, anisotropic, exponential covariance with a correlation length of 200 and 10 grid blocks in the direction parallel and perpendicular to layers, respectively. We consider both orthogonal orientations of the microlayering within the centrifugal field, parallel and perpendicular. We implement a network connectivity of 8 (communication is allowed with all surrounding blocks) to approximate three-dimensional behavior within context of a two-dimensional network, and assume that water can drain via film flow and so do not include the trapping of the defending, wetting phase. Each simulation begins with the domain completely saturated by the wetting phase with a specified A_V ranging from 0 to 1000. For $A_V = 0$, we impose a dimensionless capillary pressure at the outer surface that is sufficient to completely drain the system ($P_c = 57$). Side edges are prescribed as no flow.

[9] Non-wetting phase invasion under imposed external capillary pressure produces complicated phase structures that are nearly entirely dependent on capillary heterogeneity (Figure 2 column B). Note that color variations from dark to light in Figure 2 show the invasion order and reflect heterogeneity in the invasion process. As invasion begins, the non-wetting phase deeply penetrates along layers in the parallel system, whereas high P_s layers limit penetration into the perpendicular system. This influence of layering heterogeneity is also seen P_c (S_w) in the curves built from the simulation (Figure 3a). The parallel system drains at small P_c as continuous low P_s layers are well connected to the inlet, while the lack of continuity limits invasion in the random system and high P_s layers limit invasion in the perpendicular system. Drainage in the perpendicular system is controlled by a critical, high P_s grid block that must be spanned, after which the wetted phase saturation drops over 60% as lower P_s grid blocks drain in a large, conglomerate, cascade event. Such large cascade behavior has been observed experimentally by *Mortensen et al.* [2001], also

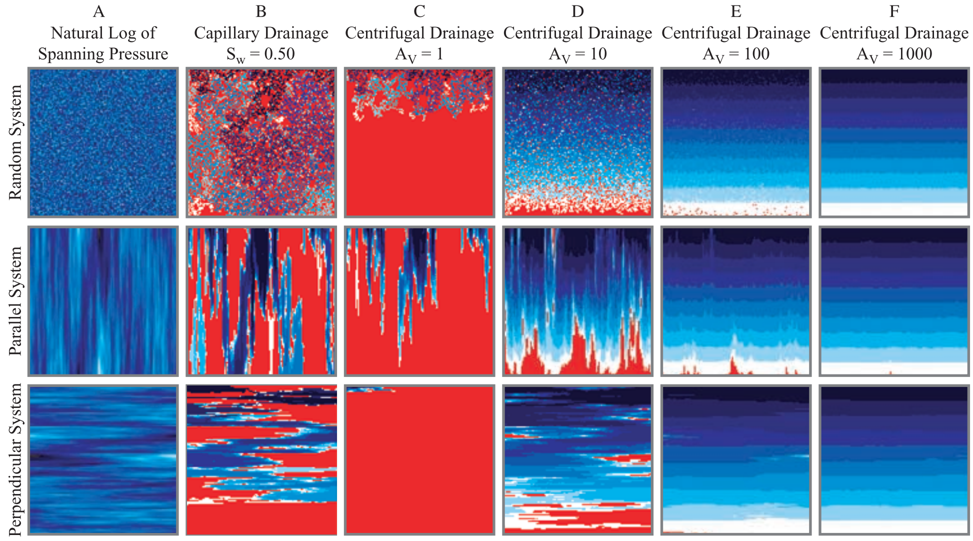

Figure 2. (a) Natural log of dimensionless spanning pressure for the random (top), parallel (middle), and perpendicular (bottom) systems. In column A, log spanning pressure increases from dark to light. Invasion history for (b) capillary drainage ($A_V = 0$ and wetting phase saturation $S_W = 0.5$) and centrifugal drainage with (c) $A_V = 1$, (d) $A_V = 10$, (e) $A_V = 100$, and (f) $A_V = 1000$. In columns B–F, non-wetting phase invasion progress from early to late is reflected by the progression of dark to light colors. Grid blocks saturated with the wetted phase are shown in red. Color contrasts at different A_V illustrate the sensitivity to capillary heterogeneity. Note non-invaded areas that appear trapped drain at higher invasion pressures.

in context of perpendicular layering, where it caused non-uniqueness in the measurement of two-phase hydraulic properties. As invasion proceeds, the parallel domain is spanned first, followed by the random system, and then the perpendicular system. In all systems, isolated regions of high P_s drain after the non-wetting phase spans the domain.

[10] In the stabilizing centrifugal field, buoyancy increases linearly with A_V but varies with the square of the distance from the inlet face. Therefore, equilibrium phase structures and invasion histories produced during centrifugal drainage vary with and distance from the inlet face. At a low A_V (Figure 2 column C), centrifugal invasion is similar to capillary invasion, and phase structures tend to follow heterogeneity. As A_V increases (Figure 2 column D), invasion becomes less sensitive to variability in P_s, particularly in regions close to the domain outlet. At high A_V (Figure 2 column E), buoyancy effects dominate the invasion pressure, and phase structures tend to be similar for all systems.

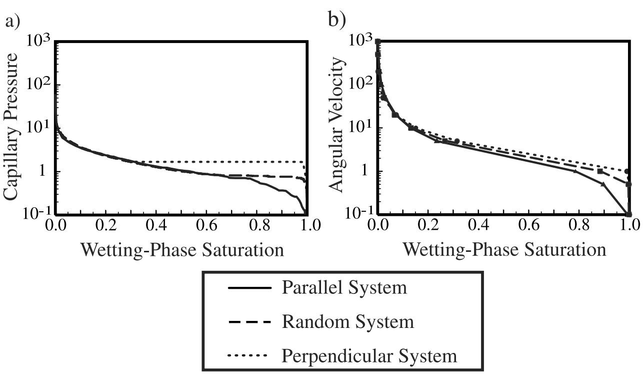

Figure 3. (a) Capillary pressure-wetting phase saturation curves for all systems. b) Angular velocity-wetting phase saturation curves for all systems.

At the very large A_V (Figure 2 column F) required to completely drain the system, phase structure evolution is essentially the same for all three capillary fields and thus is completely insensitive to heterogeneity. Invasion pressure history-saturation curves for the perpendicular system are particularly illustrative in showing how buoyancy effects increasingly dominate invasion pressures at successively higher A_V (Figure 4). At lower A_V (<100), the invasion pressure-saturation curves show a sharp decrease in saturation following the spanning of a critical grid block. The magnitude of saturation change in this drainage cascade decreases from ~60% at $A_V = 0$, to ~ 20% at $A_V = 5$, to ~ 1% at $A_V = 50$, as buoyancy stabilization begins to overwhelm capillary heterogeneity. At higher A_V ($\geq$100), drainage cascades disappear, and buoyancy dominates invasion pressures.

[11] The differences between capillary and centrifugal invasion can be illustrated further with the P_s (S_w) relationship that records the P_s values of invaded cells (Figure 5). Capillary invasion in the perpendicular system (Figure 5a) proceeds through a series of cascades that follow the

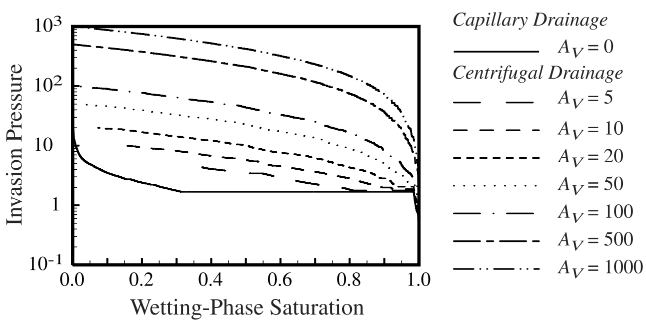

Figure 4. Invasion pressure-wetting phase saturation curves for the perpendicular system.

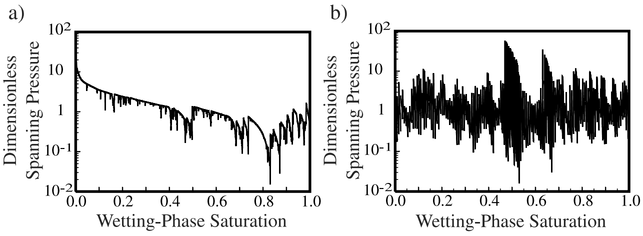

Figure 5. Spanning pressure histories for the perpendicular system during (a) capillary invasion (A_V = 0) and (b) centrifugal invasion (A_V = 1000).

spanning of high P_s cells and reflects the evolution of a complicated phase structure. The P_s history during centrifugal invasion at A_V = 1000 (Figure 5b) reflects the row by row invasion of grid blocks. Within each row, blocks are sequentially spanned from low to high P_s. As a final comparison, an angular velocity-saturation relationship [A_V (S_w)] can be built across the various simulations using the equilibrium (final) wetted-phase saturation at a specified A_V (Figure 3b). We see that although the overall trends are similar for P_c (S_w), the curves for $A_V(S_w)$ have a steeper slope and reach zero saturation at a pressure difference that is roughly two orders of magnitude greater than in the capillary invasion case.

[12] Here we have considered large systems relative to the centrifugal rotor arm length, e.g., $r_o - r_i \sim r_i$. For small systems ($r_o - r_i \ll r_i$), buoyancy increases nearly linearly with the distance from the inlet face, and phase structures will be similar to those produced in gravitational fields. *Ioannidis et al.* [1996] considered capillary drainage of random systems in the presence of increasing gravity forces. Their results also indicate decreasing sensitivity to capillary heterogeneity as gravity forces are increased.

4. Conclusions/Implications

[13] Although centrifugal methods are appealing because of greatly reduced equilibrium times, care must be taken in the design and interpretation of centrifuge experiments. Our results illustrate significant differences between phase structures developed in a centrifugal field and those developed by capillary forces alone. Because equilibrium phase structures will be dissimilar, it must be recognized that petrophysical properties (e.g., pressure-saturation relationships, relative permeability, electrical resistivity, and transport characteristics) of small samples measured in a centrifugal field will not be directly equivalent to those measured in the presence of capillary and gravity forces alone. The extent of errors in centrifuge-measured properties remains unknown and requires further study. However, with careful design, appropriately scaled systems for process-based studies can be constructed such that representative phase structure is either preserved or controlled in a centrifugal experiment. On the one hand, it will not be possible to construct a single scaled system for use at a variety of angular velocities that will maintain the same phase structure in context of capillary heterogeneity. On the other hand, a single scaled system can be used at a variety of angular velocities to vary the intrinsic nature of the phase structure in a systematic fashion. Finally, we note that while our simple study considered only stabilized invasion to an equilibrium, non-flowing state, in destabilized or flowing systems, phase structure will also be influenced by the angular velocity and must be properly interpreted to be of relevance to naturally occurring situations.

[14] **Acknowledgments.** The authors are grateful to two anonymous reviewers whose comments improved the quality of this manuscript. RMH and EDM acknowledges funding from the Environmental Systems Research and Analysis program at the Idaho National Engineering and Environmental Laboratory under DOE Idaho Operations Office Contract DE-AC07-99ID13727 BBWI. RJG acknowledges funding from the U.S. Dept. of Energy's Office of Basic Energy Research Geoscience Program under contract DE-AC04-94AL85000 to Sandia National Laboratories. JMS acknowledges support from the New Mexico Bureau of Geology and Mineral Resources.

References

Conca, J. L., and J. V. Wright, Diffusion coefficients in gravel under unsaturated conditions, *Water Resour. Res.*, *26*, 1055–1066, 1990.
Conca, J. L., and J. V. Wright, Flow and diffusion in unsaturated gravel, soil and whole rock, *Applied Hydrogeology*, *1*, 5–24, 1992.
Ewing, R. P., and B. Berkowitz, A generalized growth model for simulating initial migration of dense non-aqueous phase liquids, *Water Resour. Res.*, *34*(4), 611–622, 1998.
Forbes, P. L., Simple and accurate methods for converting centrifuge data into drainage and imbibition capillary pressure curves, *The Log Analyst*, *35*, 31–53, 1994.
Gamerdinger, A. P., and D. I. Kaplan, Application of a continuous-flow centrifugation method for solute transport in disturbed, unsaturated sediments and illustration of mobile-immobile water, *Water Resour. Res.*, *36*, 1747–1755, 2000.
Griffioen, J. W., and D. A. Barry, Centrifuge modeling of unstable infiltration and solute transport, *J. Geotech. Geoenviron. Eng.*, *125*(7), 556–565, 1999.
Glass, R. J., S. H. Conrad, and L. Yarrington, Gravity-destabilized nonwetting phase invasion in macroheterogeneous porous media: Near-pore-scale macro modified invasion percolation simulation of experiments, *Water Resour. Res.*, *37*(5), 1197–1207, 2001.
Hassler, G. L., and E. Brunner, Measurement of capillary pressures in small core samples, *Transactions, AIME*, *160*, 114–123, 1945.
Ioannidis, M. A., I. Chatzis, and F. A. L. Dullien, Macroscopic percolation model of immiscible displacement: Effects of buoyancy and spatial structure, *Water Resour. Res.*, *32*(11), 3297–3310, 1996.
Kueper, B. H., and D. B. McWhorter, The use of macroscopic percolation theory to construct large-scale capillary pressure curves, *Water Resour. Res.*, *28*(9), 2425–2436, 1992.
Levy, L. C., P. J. Culligan, and J. T. Germaine, Use of the geotechnical centrifuge as a tool to model dense nonaqueous phase liquid migration in fractures, *Water Resour. Res.*, *38*(8), doi:10.1029/2001WR000660, 2002.
Mortensen, A. P., R. J. Glass, K. Hollenbeck, and K. H. Jensen, Visualization of micro-scale phase displacement processes in retention and outflow experiments: Nonuniqueness of unsaturated hydraulic properties, *Water Resour. Res.*, *37*(6), 1627–1640, 2001.
Nimmo, J. R., J. Rubin, and D. P. Hammermeister, Unsaturated flow in a centrifugal field: Measurement of hydraulic conductivity and testing of Darcy's law, *Water Resour. Res.*, *23*, 124–134, 1987.
Savvidou, C., and P. J. Culligan, The application of centrifuge modeling to geo-environmental problems, *Proc. Inst. Civ. Engrs., Geotech. Eng.*, *131*(3), 152–162, 1998.
Wilkinson, D., and J. F. Willemsen, Invasion percolation, a new form of percolation theory, *J. Phys. A Math. Gen.*, *16*, 3365–3376, 1983.

R. M. Holt, Department of Geology and Geological Engineering, The University of Mississippi, University, MS 38677. (rmholt@olemiss.edu.)
R. J. Glass, Flow Visualization and Processes Laboratory, Sandia National Laboratories, Albuquerque, NM 87185–0735, USA. (Rjglass@sandia.gov.)
J. M. Sigda, New Mexico Bureau of Geology and Mineral Resources, New Mexico Tech., Albuquerque, NM 87106. (Jsigda@gis.nmt.edu.)
E. D. Mattson, Geosciences Research Department, INEEL, Idaho Falls, ID 83415-2107. (Matted@inel.gov.)